

Photocatalytic degradation of methylene blue dye under visible light irradiation using In/ZnO nanocomposite

ES Baeissa

Chemistry Department, Faculty of Science, King Abdulaziz University, Saudi Arabia

Abstract

A sol-gel method was used to prepare ZnO nanoparticles, and a photo-assisted deposition method was used to deposit indium into the surface of ZnO nanoparticles. BET, XRD, XPS, PL, UV-Vis and TEM measurements were used to characterize the ZnO and Pt/ZnO nanoparticles. The photocatalytic oxidation of methylene blue dye under visible light irradiation was used to determine the photocatalytic performance of the prepared nanoparticles. The results demonstrated that the indium was well dispersed on the surface of the ZnO nanoparticles. Additionally, the surface area of the In/ZnO nanoparticles was smaller than that of the ZnO nanoparticles because some of the pores of the ZnO nanoparticles were blocked by the deposited In metal. The In/ZnO nanoparticles (0.6 wt%) exhibited the lowest band gap and the highest photocatalytic activity for the methylene blue dye. The photocatalytic performance of the 0.6 wt% In/ZnO nanoparticles was stable after the nanoparticles were reused five times for the oxidation of methylene blue dye.

Introduction

In recent years, the contamination of surface and ground water has increased due to population growth. The main sources of environmental contamination are organic dyes used in the food and textile industries due to their high toxicity and their non-biodegradability, which have carcinogenic effects on humans. MB dye is used by different industries, for example, as a dye in silk; as a food colouring additive; and as a dye in wool, leather, cotton, jute, and paper [1-3]. Methylene blue dyes have strong effects on the immune and reproductive systems and exhibit potential carcinogenic and genotoxic effects [4,5]. Thus, these hazardous dyes must be removed from industrial effluents. Many methods, such as biological treatment [6,7], adsorption [8], and photocatalysis [9-13], have been used for removal of these dyes from industrial effluents. The use of photocatalysts to degrade organic compounds in contaminated air or water or to convert them into harmless chemicals has been extensively studied to decrease the damage caused by organic dye pollution to the environment and humans [14]. Therefore, heterogeneous photocatalysis is an interesting area of research because the method allows for complete mineralization of these environmentally hazardous dyes [13]. Among a variety of photocatalysts, TiO₂ is the most common photocatalyst due to its non-toxicity, good activity and high resistance to corrosion. One of the disadvantages for the use of titanium dioxide is its absorption in the UV region, which represents approximately 5% of sunlight. Therefore, the absorption of the photocatalyst must be altered to move it from the UV to visible region. Many methods have been studied to extend the absorption of photocatalysts from the UV to the visible region, such as variation of the titanium dioxide by metal or non-metal [14,15]. Other attempts have focused on preparing new photocatalysts, such as multi-metal oxide photocatalysts [16-19]. Zinc Oxide (ZnO) belongs to a category of n-type semiconductors having wide energy band gap of 3.37 eV. Recently, ZnO has attracted much attention as a promising photocatalytic material for removal of organic pollutants, which present in wastewater, all because of its high catalytic activity, moderate preparation cost and environmentally benign nature [20-

23]. Nanoscale ZnO particles possess significant surface area and large number of active sites ensure increased surface catalyzed reaction rates thus promoting photocatalysis [24]. However, the large energy band gap of ZnO permits electronic excitations only with photons having energy below 400 nm (UV spectrum). High degree of recombination of photogenerated species is another limitation associated with ZnO which is responsible for low photocatalytic activity [25-28]. These shortfalls can be remediated by modifying ZnO such as to extend its absorption threshold to the visible spectrum and limiting the rate of electron/hole pair recombination. Different attempts were achieved recently to improve the activity of ZnO photocatalyst. Development of nanoscale core/shell materials is a worth mentioning technique receiving considerable attraction [29,30]. The functional groups attached on the outer shell provide with the surface charge and reactivity to the surface and may also help to stabilize and provide equal dispersion of the core material. On other hand the characteristic catalytic, optoelectronic or magnetic properties of the shell may also be imparted to the core particles. The main aim to synthesize core/shell structured materials is to achieve a mix of the best qualities of the components in the composite materials. A number of studies focused on the synthesis of composite materials such as; NiO [31], V₂O₅ [32], TiO₂ [33], Fe₂O₃ [34], Pt [35], and Ag [36-37] with SiO₂ coatings have been reported. SiO₂ has been given significant consideration as a shell candidate based on easy preparation, environmental friendliness and conformity with most other materials, which provides and ample motivation to synthesize the ZnO and SiO₂ core/shell structured composite with expectation of achieving novel photocatalytic

Correspondence to: Elham Baeissa, Chemistry Department, Faculty of Science, King Abdulaziz University, P.O. Box 80203 Jeddah 21589, Saudi Arabia, Tel.: +966-6400000; Fax: +966-2-6952292 E-mail: elhambaeissa@gmail.com

Key words: ZnO, indium doping, photocatalyst, methylene blue dye oxidation

Received: October 14, 2016; **Accepted:** October 29, 2016; **Published:** October 31, 2016

properties from their synergic interaction. Surface modification by metal doping of photocatalytically active material has shown much promise towards increase in photocatalytic efficiency. The dopant ions act as electron sinks thus prevent the recombination of photogenerated holes with electrons, therefore, charge separation will be increased [38-41]. The physicochemical properties of ZnO nanoparticles can be altered by doping with mixed metal oxides to facilitate charge-transfer and promote its photocatalytic applications. Metal ions for instance, Iron (Fe) [42] and silver (Ag) [43,44] when used as dopants have been reported to improve the photocatalytic activity of ZnO. A number of controlling factors such as particle dimensions, number of actives sites, energy band gap, and stability of photogenerated species can decide the efficiency of a photocatalyst [45]. Researchers have investigated alternative routes such as multicomponent oxide catalysts, doping and altering synthesis techniques to add desired characteristics to the catalysts of choice [46-50]. However, the above methods required complicated procedures, special equipment or organometallic precursors. Therefore, the great challenge of fabricating ZnO nanocrystals with uniform size and well-defined crystal shape still remains. Thus, the efficiency of visible-light-harvesting was increased by increasing the optical path length of photons and surface area, which can be achieved by preparing a mesoporous semiconductor/metal composite. In this work, In/ZnO nanoparticles were prepared by a sol-gel method. The photocatalytic performance of the prepared materials was studied by the photocatalytic degradation of methylene blue dye using visible light irradiation.

Experimental

Preparation of photocatalyst

ZnO nanoparticles were synthesized via a sol-gel technique. In a typical procedure, 20 ml zinc methoxide was mixed with methyl alcohol, ultra pure water (H_2O) and nitric acid (HNO_3) under vigorous stirring for 1 hr. The prepared samples were aged at room temperature till form a gel. Finally, the samples were evaporated and dried at 80 °C, followed by calcination at 550°C for 5 h in air.

A photo-assisted deposition method was used to prepare In/ZnO. Typically, ZnO was impregnated in an aqueous solution of $InCl_3 \cdot 4H_2O$ (containing 0.2, 0.4, 0.6 or 0.8 wt% of In). Then, the resulting mixture was exposed to UV irradiation for 24 h. The obtained sample was dried for 24 h at 60°C.

Characterization techniques

A Bruker axis D8 instrument with Cu K α radiation ($\lambda = 1.540 \text{ \AA}$) was used for X-ray diffraction (XRD) analysis, which was performed at room temperature. N_2 adsorption measurements were conducted using a Nova 2000 series Chromatech apparatus at 77K to calculate the surface area. The samples were treated for two hours under vacuum at 100°C before taking the measurements. UV-visible diffuse reflectance spectroscopy (UV-Vis-DRS) was used to display the performance of the sample band gaps of samples. The spectroscopy was conducted in air at room temperature using a UV/Vis/NIR spectrophotometer (V-570, JASCO, Japan) in the wavelength range of 200 to 800 nm. A JEOL JEM-1230 microscope was used for transmission electron microscopy (TEM). The samples were entirely placed in a suspension of ethanol and then ultrasonicated for half an hour. A small amount of solution was placed on a copper grid, coated with carbon and left to dry. After the solution was dry, the sample was loaded into the TEM. A Shimadzu RF-5301 fluorescence spectrophotometer was used for recording the photoluminescence (PL) emission spectra.

Photocatalysis experiment

A xenon lamp (300 W power and 0.96 W/cm^2 intensity with a cutoff filter of 420 nm) was used to study the photocatalytic degradation of methylene blue dye. Prior to the photocatalytic test, the photocatalyst was suspended in an aqueous solution of methylene blue dye in a 500 ml reactor. Then, the obtained mixture was stirred for 30 min in the dark to establish the adsorption-desorption equilibrium. At different time intervals, samples from the mixture were taken and filtered for analysis. The absorbance of the samples were analyzed using a spectrophotometer.

Results and discussion

Structural, morphological and compositional characterizations

Figure 1 shows the XRD patterns of the ZnO and In/ZnO nanoparticles. The results reveal that all samples were mainly composed of ZnO, which indicates that the lack of diffraction peaks due to indium in the patterns of the In/ZnO samples, because the indium wt% was below the XRD detection limit or because indium was well dispersed on surface of ZnO nanoparticles.

Figure 2 shows TEM images of the ZnO and In/ZnO nanoparticles. The results show that increased indium wt%, the indium dispersion increased on the surface of the ZnO nanoparticles. Additionally, increased indium wt% up to 0.6% increased the homogeneity of the In particle size on the surface of the ZnO nanoparticles. This homogeneity decreased at higher concentrations of In, *i.e.*, 0.6 wt%, which suggests that there is an optimum content for the deposition of indium ions that controls the size and homogeneity of the doped indium (Figure 3).

Surface area analysis

BET surface area of ZnO and In/ZnO nanoparticles are presented in Table 1. The S_{BET} values for ZnO 0.2 wt% In/ZnO, 0.4 wt% In/ZnO, 0.6 wt% In/ZnO and 0.8 wt% In/ZnO were determined to be 50, 46, 44, 40 and $38 \text{ m}^2/\text{g}$, respectively. The BET surface area of In/ZnO nanoparticle was lower than that of the ZnO sample because some of the pores were blocked by the deposited of indium.

Optical characterization

Figure 4 shows the UV-Vis diffuse reflectance spectra of the ZnO and In/ZnO nanoparticles. The results demonstrate that the deposition of indium onto the ZnO surface led to a shift in the absorption edge of ZnO from 387 nm to 454 nm. The UV-Vis spectra were used to calculate the direct band gaps of the ZnO and Pt/ZnO nanoparticles.

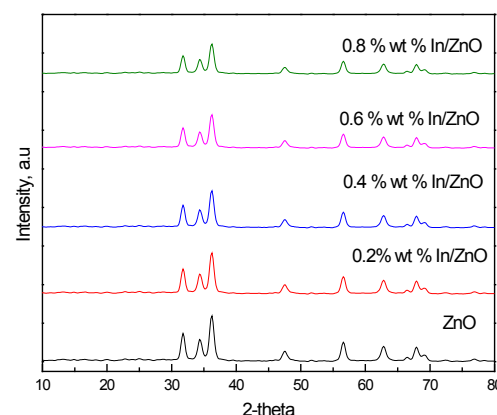


Figure 1. XRD patterns of ZnO and In/ZnO nanoparticles.

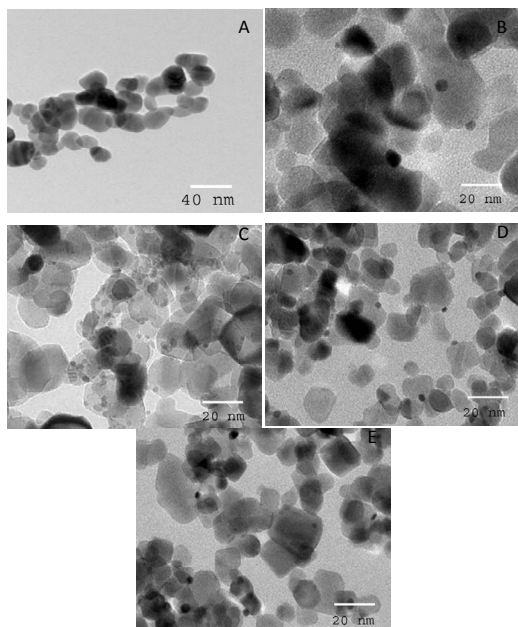


Figure 2. TEM images of ZnO and In/ZnO nanoparticles, where the In wt% is 0.0 (A); 0.2 (B); 0.4 (C); 0.6 (D) and 0.8 (E).

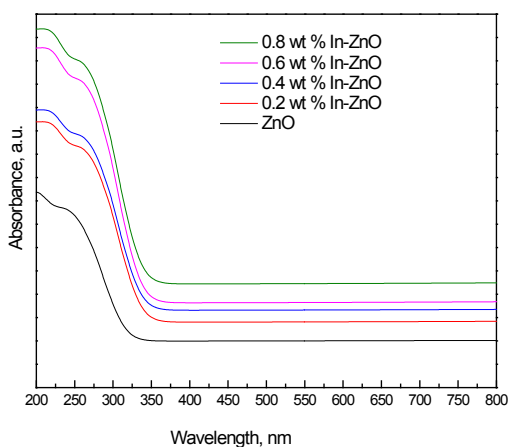


Figure 3. UV-Vis absorption spectra of ZnO and In/ZnO nanoparticles.

Table 1. BET surface area of ZnO and In/ZnO nanoparticles.

Sample	S_{BET} (m ² /g)
ZnO	50.00
0.2 wt% In/ZnO	46.00
0.4 wt% In/ZnO	44.00
0.6 wt% In/ZnO	40.00
0.8 wt% In/ZnO	38.00

The band gap energies were calculated using the following equation:

$$E_g = 1239.8/\lambda$$

where E_g is the band gap (eV) and λ is the wavelength (nm) of the absorption edges in the spectrum; the results are tabulated in Table 2. The results reveal that increasing the In wt% from 0.2 wt% to 0.6 wt% decreased the band gap from 3.2 eV to 2.73 eV, respectively. However, there was no significant effect on the band gap at a high wt% of In (greater than 0.6). Therefore, there is an optimum content of deposited In that controls the band gap.

We investigated the separation and recombination of photogenerated charge carriers and the transfer of the photogenerated electrons and holes by gathering photoluminescence (PL) emission spectra. The results indicate that an increase in the wt% of In deposited on the ZnO nanoparticles from 0.2 wt% to 0.6 wt% led to decreased PL intensity. However, there was no significant effect on the PL intensity at a high in wt% (above 0.6), as shown in Figure 4. Therefore, there is an optimum content of deposited in that yields the carrier lifetime required for e-h recombination, which is in agreement with the UV-Vis results.

Photocatalytic activities

Figure 5 shows the effect of the In wt% on the photocatalytic activity of ZnO and In/ZnO nanoparticles for the oxidation of methylene blue dye under visible light irradiation. The experiment was performed under the following conditions: methylene blue dye concentration of 100 ppm, methylene blue dye volume of 1000 ml and photocatalyst

Table 2. Band gap energies ZnO and In/ZnO nanoparticles.

Sample	Band gap energy, eV
ZnO	3.20
0.2 wt% In/ZnO	2.95
0.4 wt% In/ZnO	2.83
0.6 wt% In/ZnO	2.73
0.8 wt% In/ZnO	2.62

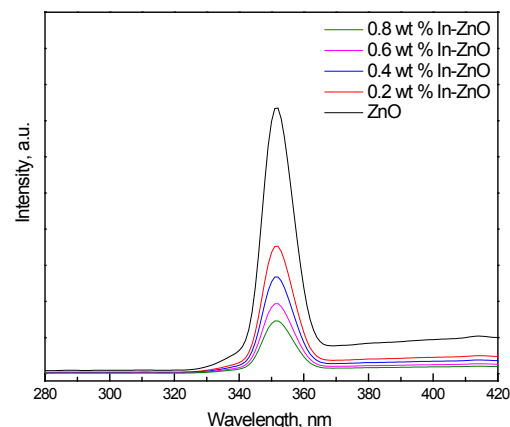


Figure 4. PL spectra of ZnO and In/ZnO nanoparticles.

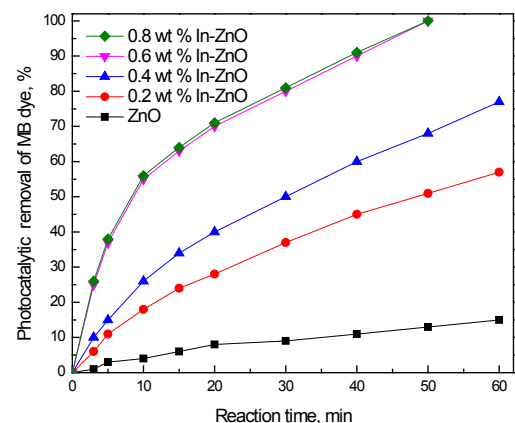


Figure 5. Effect of the In wt% on the photocatalytic activity of ZnO and In/ZnO nanoparticles for the oxidation of methylene blue dye.

weight of 0.75 g. The results reveal that the photocatalytic activity increased from 15 to 100% as the indium wt% increased from 0 to 0.6 wt%. However, further increasing the indium wt% above 0.6 wt% has no significant effect on photocatalytic activity.

Figure 6 shows the effect the loading of the 0.6 wt% In/ZnO sample on the photocatalytic oxidation of methylene blue dye solution under visible light irradiation; the experiment was performed under the following conditions: methylene blue dye concentration of 100 ppm, methylene blue dye volume of 1000 ml and a 0.6 wt% In/ZnO nanoparticles photocatalyst. The results reveal that photocatalytic performance, in terms of the percentage, increased after 50 min from 97% to 100% with increased weight of the photocatalyst from 0.50 g/l to 0.75 g/l. The reaction time required to complete the oxidation of methylene blue dye decreased to 30 min as the weight of the photocatalyst was increased to 1.0 g/l. However, the reaction time required to complete the oxidation of methylene blue dye increased again to 45, and 55 min as the weight of the photocatalyst increased to 1.25 g/l and 1.50 g/l, respectively. Therefore, the optimum weight of the photocatalyst is 1.0 g/l.

Figure 7 shows the results obtained regarding the recycling and reuse of the photocatalysts for photocatalytic oxidation of methylene blue dye solutions. The experiment was carried out under the following conditions: reaction time of 30 min, methylene blue dye solution concentration of 100 ppm and 1.0 g/l of the 0.6 wt% In/ZnO sample.

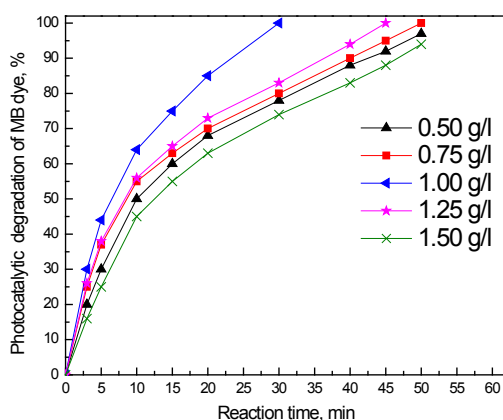


Figure 6. Effect of the loading of the 0.6 wt% In/ZnO sample on the photocatalytic oxidation of methylene blue dye.

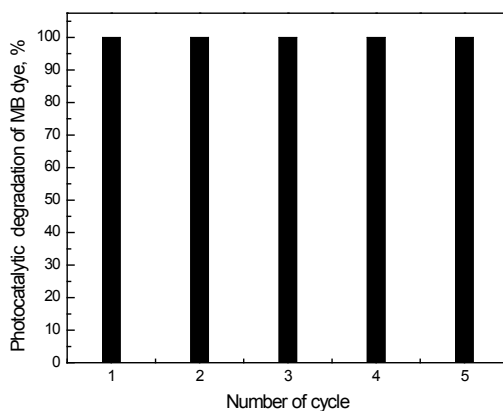


Figure 7. Recycling and reuse of 0.6 wt% In/ZnO photocatalysts for the photocatalytic oxidation of methylene blue dye solutions.

ZnO nanoparticle. The results show that the photocatalytic activity remained nearly unchanged after five uses, which indicates that the photocatalyst is stable in the photocatalytic oxidation of methylene blue dye solutions. Therefore, this photocatalyst can be separated and recycled while maintaining its stability, making it a promising material for environmental remediation.

Conclusions

In summary, a In/ZnO nanoparticle photocatalyst was successfully synthesized and was demonstrated to be a promising catalyst due to its high efficiency in oxidizing methylene blue dye under visible light. The band gap of the ZnO_{photocatalyst} could be controlled by controlling the weight percent of indium that is deposited onto the surface of the photocatalyst. The results of photocatalytic studies reveal that the highest photocatalytic activity and stability were obtained for the 0.6 wt% In/ZnO nanoparticle photocatalyst, which can be used to oxidize 100% of methylene blue dye after 30 min.

References

- Sarmah S, Kumar A (2008) Photocatalytic activity of polyaniline-TiO₂ nanocomposites. *Indian J Phys.* 85: 713–726.
- Srivastava S, Sinha R, Roy D (2004) Toxicological effects of malachite green. *Aquat Toxicol* 66: 319–329. [Crossref]
- Cheng W, Wang SG, Lu L, Gong WX, Liu XW, et al. (2008) Interaction between congo red and copper in a binary adsorption system: Spectroscopic and kinetic studies. *Biochem Eng J* 538–546.
- Rao KV (1995) Inhibition of DNA synthesis in primary rat hepatocyte cultures by malachite green: a new liver tumor promoter. *Toxicol Lett* 81: 107–113. [Crossref]
- Alderman DJ, Clifton-Hadley RS (1993) Malachite green: a pharmacokinetic study in rainbow trout, *Oncorhynchus mykiss* (Walbaum). *J Fish Dis* 16: 297–311.
- Ramezani S, Pourbabaei AA, Javaheri JA, Bioremed J (2013) Photocatalytic performance of ZnO nanomaterials for self-sensitized degradation of malachite green dye under solar light. *Biodegrad* 4: 1000175.
- Wang J, Qiao M, Wei K, Ding J, Liu Z, et al. (2011) Decolorizing activity of malachite green and its mechanisms involved in dye biodegradation by Achromobacter xylosoxidans MG. *J Mol Microbiol Biotechnol* 20: 220–227. [Crossref]
- Mittal A (2006) Adsorption kinetics of removal of a toxic dye, Malachite Green, from wastewater by using hen feathers. *J Hazard Mater* 133: 196–202. [Crossref]
- Sayilan M, Asilturk M, Tatar P, Kiraz N, Arpac E, et al. (2007) Preparation of reusable photocatalytic filter for degradation of Malachite Green dye under UV and vis-irradiation. *J Hazard Mater* 148: 735–744.
- Chen CC, Lu CS, Chung YC, Jan JL (2007) UV light induced photodegradation of malachite green on TiO₂ nanoparticles. *J Hazard Mater* 141: 520–528. [Crossref]
- Pare B, Sarwan B, Jonnalagadda SB (2011) Photocatalytic mineralization study of malachite green on the surface of Mn-doped BiOCl activated by visible light under ambient condition. *Appl Surf Sci* 258: 247–253.
- Liu Y, Ohko Y, Zhang R, Yang Y, Zhang Z (2010) Degradation of malachite green on Pd/WO₃ photocatalysts under simulated solar light. *J Hazard Mater* 184: 386–391. [Crossref]
- Prado AG, Costa LL (2009) Photocatalytic decoloration of malachite green dye by application of TiO₂ nanotubes. *J Hazard Mater* 169: 297–301. [Crossref]
- Herrmann JM, Disdier M, Pichat P (1984) Effect of chromium doping on the electrical and catalytic properties of powder titania under UV and visible illumination. *Chemical Physics Letters* 108: 618–622.
- Cheng ZJ, Liu TY, Chen XY, Gan HX, Zhang FW, et al. (2012) Study on the electronic structures of the reduced anatase TiO₂ by the first-principle calculation. *Journal of Physics and Chemistry of Solids* 73: 302–307.
- Tang J, Zou Z, Ye J (2004) Efficient photocatalytic decomposition of organic contaminants over CaBi₂O₄ under visible-light irradiation. *Angew Chem Int Ed Engl* 43: 4463–4466. [Crossref]
- Li ZH, Dong Z, Zhang YF, Dong TT, Wang XX, et al. (2008) Effect of M2+ (M= Zn

- and Cu) Dopants on the Electronic Structure and Photocatalytic Activity of In (OH)_y S_z Solid Solution. *Journal of Physical Chemistry C* 112: 16046.
18. Shi HF, Li ZS, Kou J, Ye JH, Zou ZG (2011) Facile synthesis of single-crystalline Ag₂V₄O₁₁ nanotube material as a novel visible-light-sensitive photocatalyst. *Journal of Physical Chemistry C* 115: 145.
 19. Cheng HF, Huang BB, Liu YY, Wang ZY, Qin XY, et al. (2012) An anion exchange approach to Bi₂WO₆ hollow microspheres with efficient visible light photocatalytic reduction of CO₂ to methanol. *Chemical Communications* 48: 9729.
 20. Hariharan C (2006) Photocatalytic degradation of organic contaminants in water by ZnO nanoparticles: revisited. *Appl Catal A Gen* 304: 55–61.
 21. Mrowetz M, Sellin, E (2006) Photocatalytic degradation of formic and benzoic acids and hydrogen peroxide evolution in TiO₂ and ZnO water suspensions. *J Photochem Photobiol A: Chem* 180: 15–22.
 22. Pauporte T, Rathousky J (2007) Electrodeposited mesoporous ZnO thin films as efficient photocatalysts for the degradation of dye pollutants. *J Phys Chem C* 111: 7639–7644.
 23. Yu J, Yu X (2008) Hydrothermal synthesis and photocatalytic activity of zinc oxide hollow spheres. *Environ Sci Technol* 42: 4902–4907. [crossref]
 24. Sun JH, Dong SY, Wang YK, Sun SP (2009) Preparation and photocatalytic property of a novel dumbbell-shaped ZnO microcrystal photocatalyst. *J Hazard Mater* 172: 1520–1526. [Crossref]
 25. Zhou M, Yu J, Cheng B (2008) Preparation, characterization and visible-light-driven photocatalytic activity of Fe-doped titania nanorods and first-principles study for electronic structures. *J of Hazard Mater B* 137: 1838.
 26. Klingshirn C (2007) ZnO: Material, physics and applications. *Chemphyschem* 8: 782–803.
 27. Singhal A, Achary S, Tyagi A, Manna A, Yusuf S (2008) Colloidal Fe-doped ZnO nanocrystals: facile low temperature synthesis, characterization and properties. *Mater Sci And Eng B* 153: 47.
 28. Estrellan C, Salim C, Hinode H (2008) Enhancement of photocatalytic activity of ZnO–SiO₂ by nano-sized Ag for visible photocatalytic reduction of Hg (II). *React Kinet Catal Lett* 98: 187.
 29. Schneider JJ (2008) Enhanced visible light photocatalysis through fast crystallization of zinc oxide nanorods. *Adv Mater* 13: 529–533.
 30. Lee HB, Yoo YM, Han YM (2006) Characteristic optical properties and synthesis of gold–silica core–shell colloids. *Scripta Mater* 55: 1127–1129.
 31. Mohamed RM, Aazam ES (2012) Influence of Cu doping on structural, optical and photocatalytic activity of SnO₂ nanostructure thin films. *Journal of Nanotechnology* art. no. 794874.
 32. Ismail AA, Ibrahim IA, Mohamed RM (2006) Enhanced nanocatalysts. *Appl Catal B Environ.* 45: 161–166
 33. Liu T, Wang XR, An Y, Zhou YS, Zhang XY, et al. (2012) Sulphasalazine in patients with rheumatoid arthritis in China: a cross-sectional study. *Beijing Da Xue Xue Bao* 44: 188–194. [Crossref]
 34. Maurice V, Georgelin T, Siaugue JM, Cabuil V (2009) Synthesis and characterization of functionalized core–shell γFe₂O₃–SiO₂ nanoparticles. *J Magn Magn Mater* 321: 1408–1413.
 35. Mohamed RM (2009) Characterization and catalytic properties of nano-sized Pt metal catalyst on TiO₂–SiO₂ synthesized by photo-assisted deposition and impregnation methods. *Journal of Materials Processing Technology* 209: 577–583.
 36. Chou KS, Chen CC (2007) Fabrication and characterization of silver core and porous silica shell nanocomposite particles. *Micropor Mesopor Mater* 98: 208–213.
 37. Mohamed RM, Mkhaldia IA (2010) Characterization and catalytic properties of nano-sized Ag metal catalyst on TiO₂–SiO₂ synthesized by photo-assisted deposition and impregnation methods. *Journal of Alloys and Compounds* 501: 301–306.
 38. Height M, Pratsinis S, Mekasuwandumrong O, Praserthdam P, et al. (2006) Ag-ZnO catalysts for UV-photodegradation of methylene blue. *Appl Catal B Environ* 63: 305.
 39. Han T, Wu C, Hsieh C (2007) Hydrothermal synthesis and visible light photocatalysis of metal-doped titania nanoparticles. *J Vac Sci Technol B* 25: 430.
 40. Ullah R, Dutta J (2008) Photocatalytic degradation of organic dyes with manganese-doped ZnO nanoparticles. *J Hazard Mater* 156: 194–200. [crossref]
 41. Slama F, Ghribi F, Houas A, Barthou C, et al. (2010) Structural Properties, Conductivity, Dielectric Studies and Modulus Formulation of Ni Modified ZnO Nanoparticles. *El Mir Int J Nanoelectro and Mater* 3: 133.
 42. Mohamed RM, Al-Rayyan MA, Baeissa ES, Mkhaldia IA (2011) Preparation and characterization of platinum doped porous titania nanoparticles for photocatalytic oxidation of carbon monoxide. *Journal of Alloys and Compounds* 509 24: 2016824–6828.
 43. Ren C, Yang B, Wu M, Xu J, Fu Z, et al. (2010) Synthesis of Ag/ZnO nanorods array with enhanced photocatalytic performance. *J Hazard Mater* 182: 123–129. [crossref]
 44. Lai Y, Meng M, Yu Y (2010) One-step synthesis, characterizations and mechanistic study of nanosheets-constructed fluffy ZnO and Ag/ZnO spheres used for Rhodamine B photodegradation. *Appl Catal B Environ* 100: 491–501.
 45. Mohamed RM, McKinney DL, Sigmund WM, et al. (2012) Enhanced nanocatalysts. *Materials Science & Engineering R-Reports* 73: 1.
 46. Yuan M, Zhang J, Yan S, Luo G, Xu Q, Wang X, et al. (2011) Effect of Nd₂O₃ addition on the surface phase of TiO₂ and photocatalytic activity studied by UV Raman spectroscopy. *Journal of Alloys and Compounds* 509: 6227.
 47. Yao N, Cao S, Yeung M (2009) Mesoporous TiO₂–SiO₂ aerogels with hierarchical pore structures. *Microporous and Mesoporous Materials* 117: 570.
 48. Tel H, Altas Y, Eral M, Sert S, Cetinkaya B, Inan S (2010) Preparation of ZrO₂ and ZrO₂–TiO₂ microspheres by the sol–gel method and an experimental design approach to their strontium adsorption behaviours. *Chemical Engineering Journal* 161: 151.
 49. Yamazaki S, Fujiwara Y, Yabuno S, Adachi K, Honda K (2012) Synthesis of porous platinum-ion-doped titanium dioxide and the photocatalytic degradation of 4-chlorophenol under visible light irradiation. *Applied Catalysis B-Environmental* 121: 148.
 50. Karunakaran C, Dhanalakshmi R, Gomathisankar P (2012) Phenol-photodegradation on ZrO₂: Enhancement by semiconductors. *Spectrochim Acta A Mol Biomol Spectrosc* 92: 201–206. [crossref]